Journal of Electrical Engineering, Vol. 75, No. 4, 2024, pp. 275-284

sciendo

PAPERS

Comparative performance analysis of robust and adaptive controller for three-link robotic manipulator system

Sweta, Vinay Kumar Deolia, Jitendra Kumar

Three-link robotic manipulator systems (TLRMS) often used in automation industries offer many capabilities, but become very complex in terms of their control and operations. In order to enhance trajectory tracking in the X and Y axes, this study investigates the application of a fractional-order nonlinear proportional, integral, and derivative (FONPID) controller for a three-link robotic manipulator system (TLRMS). Using a cost function that combines the integral of square error (ISE) and the integral of absolute change in controller output (IACCO), the cuckoo search algorithm (CSA) maximises the performance of the controller. The fractional-order term enhances the robustness and the nonlinear term supports the adaptiveness of the FONPID controller. The fractional-order proportional, integral, and derivative (FOPID) and classic PID controllers are contrasted with the FONPID controller's efficacy. The findings show that the CSA-tuned FONPID performs better than the other controllers, providing more robust and accurate tracking. By demonstrating fractional-order control's promise for intricate robotic systems, this study advances the discipline.

Keywords: fractional-order operator, FOPID controller, FONPID controller, Three-link robotic manipulator system, CSA

1 Introduction and literature survey

Because of its versatility and range of motion, three-link robotic manipulators (TLRMS) are frequently employed in automation, manufacturing, and robotics research. With their three articulated joints, these manipulators can execute complex tasks including assembly, precision positioning, and object handling since they have multiple degrees of freedom (DOF) [1]. These systems can imitate human movements thanks to their greater DOF, which makes them adaptable to a wide range of industrial applications. Three-link robotic manipulators require careful consideration of kinematics, dynamics, and control methods at every stage of design and operation. The interconnected and nonlinear nature of these systems means that precise and reliable performance must be ensured through the development of efficient control algorithms. While conventional controllers, like PID, offer a straightforward approach, their inability to adequately capture the dynamics of complex systems can lead to subpar performance [2-4]. Fractional-order controllers, which incorporate non-integer order derivatives and integrals to extend standard proportional-integral-derivative (PID) control, are a recent development in control theory [5]. These controllers may be adjusted for better performance and provide more versatility. These sophisticated control strategies become more and more beneficial as robotic systems get more complicated, allowing manipulators to more precisely and dependably fulfil the needs of contemporary industrial activities [6]. Advanced robotic applications, ranging from complex assembly jobs to precision manufacturing, require three-link robotic manipulators as essential components. Multiple DOF are built into their design, giving them a wide range of motion options and operating flexibility [6]. They may be used for a wide range of jobs, from straightforward pick-and-place procedures to intricate assembly and welding, thanks to their versatility. These benefits do, however, come with more complexity, especially when it comes to kinematic and dynamic analysis [6]. In order to attain the intended results, these manipulators must be controlled effectively, particularly with regard to accuracy and repeatability. Due to their ease of use and efficiency in linear systems, traditional control techniques like PID controllers have served as the foundation for industrial robots [7]. These approaches, however, might not be adequate when dealing with coupled movements and non-linear dynamics [8]. Due to this constraint, researchers have been exploring more sophisticated control techniques, such as fractional-order controllers, which provide increased flexibility and control over the behaviour of the system. Non-integer orders are incorporated into the differentiation and integration processes via fractional-order controllers, which offers a wider control bandwidth and more precise system response customisation. Improved tracking accuracy and system stability can result from this greater control flexibility, which is important for robotic applications that is needed for precise trajectory following [9-14].

ECE Department, GLA University, Mathura (281406), India
sweta.gla@gla.ac.in, vinaykumar.deolia@gla.ac.in, jitendra.kumar@gla.ac.in

https://doi.org/10.2478/jee-2024-0034, Print (till 2015) ISSN 1335-3632, On-line ISSN 1339-309X
© This is an open access article licensed under the Creative Commons Attribution-NonCommercial-NoDerivatives License (http://creativecommons.org/licenses/by-nc-nd/4.0/).

Algorithms like the Cuckoo Search Algorithm (CSA) have become popular for optimising these controllers for complicated manipulator systems. Cuckoo-inspired nesting behaviour (CSA) is a nature-inspired optimisation strategy that has been shown to be successful in solving challenging optimisation problems. The controller parameters can be adjusted using CSA to provide the greatest performance feasible, which lowers error rates and boosts system stability [15-17]. By adding non-integer derivatives and integrals, fractional-order controllers increase the tuning flexibility of conventional PID controllers. According to research by Zhang et al. (2020), fractional-order nonlinear PID (FONPID) controllers outperform traditional PID controllers in trajectory tracking and disturbance rejection. This suggests that fractional-order control may be utilised to increase the precision of robotic manipulators. Optimisation algorithms based on natural phenomena, such as the CSA, are becoming more and more common for fine-tuning control system parameters [18]. According to Singh and Banga (2019), CSA can efficiently maximise controller gains, which will increase stability and decrease error. Their work demonstrates how adaptable and effective CSA is at solving challenging control system optimisation problems [19]. One popular performance indicator for assessing controller efficacy is the Integral of Squared Error (ISE). In their discussion of the benefits of ISE as an objective function, Patel et al. (2018) highlight how it helps reduce system error and gives a clear picture of overall performance. According to the study, ISE is a trustworthy statistic for evaluating controller efficiency. The integral of absolute change in controller output (IACCO) gauges the total variations in controller output, which reflects the smoothness of the control system [20]. In the context of robotic control systems and find that lower IACCO results in smoother control actions, which lessen system component wear and tear. When paired with ISE, this statistic offers a thorough assessment of controller performance. Robotic systems can handle nonlinearities more robustly thanks to the usage of nonlinear control elements in FONPID controllers [16, 21]. Further, some researchers investigate the advantages of nonlinear PID controllers in intricate robotic applications, demonstrating that they provide more flexibility and are better able to manage changing system dynamics. One innovative method that has produced encouraging results is the application of CSA to optimise FONPID controllers. In their demonstration of the use of CSA in fractional-order control, later studies show how the algorithm's randomization and discovery mechanisms can aid in the more efficient determination of optimal controller parameters than those found in more conventional techniques. Analysing and contrasting various controller types helps to understand their advantages and disadvantages. In a comparison analysis of FONPID and conventional PID controllers, Devbrat et al. (2024) show that fractional-order controllers, particularly in systems with complex dynamics, typically provide higher precision and control. For robotic manipulators, following their trajectory is an essential function. In their study on trajectory tracking accuracy in multi-link robotic systems, Kumar et al. (2023) show that FONPID controllers can keep accurate trajectories even when there are outside disturbances and uncertainties in the system. Robotic control can face significant challenges due to system complexity. According to studies, CSA-tuned controllers can simplify and strengthen control strategies by effectively optimising control parameters. According to their research, CSA can assist in resolving a few of the difficulties that complicated robotic systems always face. Industrial robotics applications often require high levels of precision and reliability. The study on the use of FONPID controllers in industrial environments found that the robust system dynamics handling of these controllers can reduce downtime and boost output.

The study concludes that FONPID controllers have a great deal to offer the industrial robotics community. The advantages of fractional-order controller (FOC) in terms of additional DOF in the event that a PID control operation fails are also the subject of the literature study. Adaptive approaches, like adding nonlinearity, improve the performance of FOCs even more. Control is challenging since the system is nonlinear and MIMO-coupled. While tracking planned trajectories, the FONPID control action attempts to castoff outside disturbances and sensor noise. When it comes to trajectory tracking and the X and Y movement of TLRMS based on angular position, the FONPID controller outperforms the PID and NPID controllers [5, 17, 22-29].

The following is how the research manuscript is formatted: Section 1 features an introduction and a review of the literature, while Section 2 deals with dynamic plant modelling. In section 3, the recommended controller design and CSA adjustment are shown. Section 4 provides a full description of the comparative analysis of the simulation findings. Section 5 brings the proposed work to a close.

2 Dynamic system modeling

The structural configuration of a Three-link Robotic Manipulator System (TLRMS), shown in Fig. 1, is covered in this section. At every pivot point, the system is designed to minimise friction. In order to accomplish this, a frictionless pivot mechanism is used to join the initial link to a rigid foundation. The precision and longevity of the system are enhanced by this frictionless pivot, which guarantees smooth operation and minimises wear and tear. The upper end of the first link is connected to the second link. The frictionless ball bearing used in this connection permits smooth rotation and angular movement between the two links. Making this design decision is essential to preserving the system's accuracy and lowering resistance. The third-link is correspondingly attached to the top of the second-link using a different frictionless ball-bearing mechanism. With this arrangement, the TLRMS's joints function with the least amount of resistance possible, allowing for fluid and effective movement across the board. The performance of the TLRMS is largely dependent on the use of frictionless components, which enables accurate control and minimise the need for frequent lubrication and maintenance [22, 30].

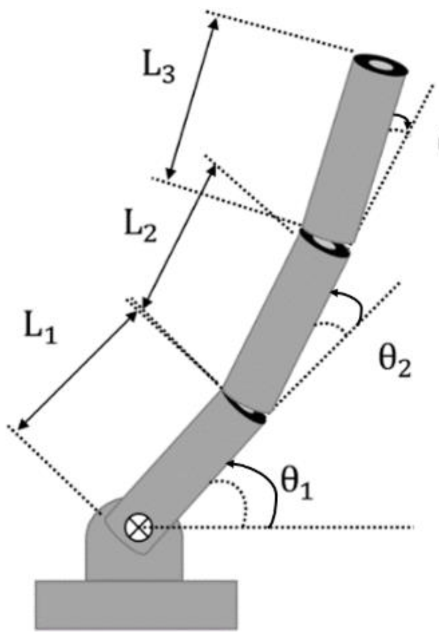

Fig. 1. Block diagram of a three-link robotic manipulator system (TLRMS) [22]

Table 1. Parametric values of mass, length and gravity used in TLRMS [22]

Parameters	L-1	L-2	L-3
mass (m_1, m_2, m_3) (kg)	0.1	0.1	0.1
length (L_1, L_2, L_3) (m)	0.8	0.4	0.4
gravity (m/s^2)	9.8	9.8	9.8

Mathematical modelling of TLRMS is illustrated in Eqn. (1) as [31],

$$\begin{bmatrix} N_{11} & N_{12} & N_{13} \\ N_{21} & N_{22} & N_{23} \\ N_{31} & N_{32} & N1_{33} \end{bmatrix} \begin{bmatrix} \ddot{\Theta}_1 \\ \ddot{\Theta}_2 \\ \ddot{\Theta}_3 \end{bmatrix} + \begin{bmatrix} P_1 \\ P_2 \\ P_3 \end{bmatrix} + \begin{bmatrix} R_1 \\ R_2 \\ R_3 \end{bmatrix} + \begin{bmatrix} g_1 \\ g_2 \\ g_3 \end{bmatrix} = \begin{bmatrix} t_1 \\ t_2 \\ t_3 \end{bmatrix} \tag{1}$$

In the above equation, the first term contains second-order derivatives of angular positions for three links $\ddot{\Theta}_i$, the second term called Centrifugal comprises the product of $\dot{\Theta}_i^2$, where $(i = 1, 2, 3)$. The third term, Coriolis, is the product of $\dot{\Theta}_i \dot{\Theta}_j$ where $(i \neq j)$. The last term comprises Θ_i attained by differentiating the potential energy stored in the links. The terms used in Eqn. (1) are provided as follows in Eqns. (2)-(18).

$$\begin{aligned} N_{11} = {} & (m_1 + m_2 + m_3)L_1^2 + (m_2 + m_3)L_2^2 \\ & + m_3 L_3^2 + 2m_3 L_1 L_3 \cos(\Theta_2 + \Theta_3) \\ & + 2(m_2 + m_3)L_1 L_2 \cos(\Theta_2) + 2m_3 L_2 L_3 \cos(\Theta_3) \end{aligned} \tag{2}$$

$$\begin{aligned} N_{12} = {} & (m_2 + m_3)L_2^2 + m_3 L_3^2 \\ & + m_3 L_1 L_3 \cos(\Theta_2 + \Theta_3) \\ & + (m_2 + m_3)L_1 L_2 \cos(\Theta_2) + 2m_3 L_2 L_3 \cos(\Theta_3) \end{aligned} \tag{3}$$

$$\begin{aligned} N_{13} = {} & m_3 L_3^2 + m_3 L_1 L_3 \cos(\Theta_2 + \Theta_3) \\ & + m_3 L_2 L_3 \cos(\Theta_3) \end{aligned} \tag{4}$$

$$\begin{aligned} N_{21} = {} & m_2 L_2^2 + m_3 L_2^2 + m_3 L_3^2 \\ & + m_3 L_1 L_3 \cos(\Theta_2 + \Theta_3) + m_2 L_1 L_2 \cos(\Theta_2) \\ & + m_3 L_1 L_2 \cos(\Theta_2) + 2m_3 L_2 L_3 \cos(\Theta_3) \end{aligned} \tag{5}$$

$$\begin{aligned} N_{22} = {} & m_2 L_2^2 + m_3 L_2^2 + m_3 L_3^2 \\ & + 2m_3 L_2 L_3 \cos(\Theta_3) \end{aligned} \tag{6}$$

$$N_{23} = m_3 L_3^2 + m_3 L_2 L_3 \cos(\Theta_3) \tag{7}$$

$$\begin{aligned} N_{31} = {} & m_3 L_3^2 + m_3 L_1 L_3 \cos(\Theta_2 + \Theta_3) \\ & + m_3 L_2 L_3 \cos(\Theta_3) \end{aligned} \tag{8}$$

$$N_{32} = m_3 L_3^2 + m_3 L_2 L_3 \cos(\Theta_3) \tag{9}$$

$$N_{33} = m_3 L_3^2 \tag{10}$$

Centrifugal terms are defined as:

$$\begin{aligned} P_1 = {} & -L_1(m_3 L_3 \sin(\Theta_2 + \Theta_3) + m_2 L_2 \sin(\Theta_2) \\ & + m_3 L_2 \sin(\Theta_2))\dot{\Theta}_1^2 \\ & - m_3 L_3 (L_1 \sin(\Theta_2 + \Theta_3) + L_2 \sin(\Theta_3))\, \dot{\Theta}_3^2 \end{aligned} \tag{11}$$

$$\begin{aligned} P_2 = {} & L_1(m_3 L_3 \sin(\Theta_2 + \Theta_3) + m_2 L_2 \\ & + m_3 L_2 \sin(\Theta_2))\dot{\Theta}_1^2 \\ & - m_3 L_2 L_3 \sin(\Theta_3)\, \dot{\Theta}_3^2 \end{aligned} \tag{12}$$

$$\begin{aligned} P_3 = {} & m_3 L_3 (L_1 \sin(\Theta_2 + \Theta_3) + L_2 \sin(\Theta_3))\dot{\Theta}_1^2 \\ & + m_3 L_2 L_3 \sin(\Theta_3)\, \dot{\Theta}_2^2 \end{aligned} \tag{13}$$

Coriolis terms are defined as:

$$\begin{aligned} R_1 = {} & -2L_1(m_3 L_3 \sin(\Theta_2 + \Theta_3) \\ & + (m_2 + m_3)L_2 \sin(\Theta_2))\, \dot{\Theta}_1 \dot{\Theta}_2 \\ & - 2m_3 L_3 (L_1 \sin(\Theta_2 + \Theta_3) + L_2 \sin(\Theta_3))\, \dot{\Theta}_2 \dot{\Theta}_3 \\ & - 2m_3 L_3 (L_1 \sin(\Theta_2 + \Theta_3) + L_2 \sin(\Theta_3))\dot{\Theta}_1 \dot{\Theta}_3 \end{aligned} \tag{14}$$

$$R_2 = -2m_3L_2L_3\sin(\Theta_3)\,\dot{\Theta}_1\dot{\Theta}_3 - 2m_3L_2L_3\sin(\Theta_3)\,\dot{\Theta}_3\dot{\Theta}_2 \quad (15)$$

$$R_3 = 2m_3L_2L_3\sin(\Theta_3)\,\dot{\Theta}_1\dot{\Theta}_2 \quad (16)$$

The terms having potential energy are defined as:

$$g_1 = (m_1 + m_2 + m_3)\,g\,L_1\cos(\Theta_1) + (m_2 + m_3)\,g\,L_2\cos(\Theta_1 + \Theta_2) + m_3gL_3\cos(\Theta_1 + \Theta_2 + \Theta_3) \quad (17)$$

$$g_2 = (m_2 + m_3)\,g\,L_2\cos(\Theta_1 + \Theta_2) + m_3gL_3\cos(\Theta_1 + \Theta_2 + \Theta_3) \quad (18)$$

$$g_3 = m_3gL_3\cos(\Theta_1 + \Theta_2 + \Theta_3) \quad (19)$$

3 FONPID controller design and gains tuning using CSA

This section compares the performance of FOPID and traditional PID controllers with a FONPID controller on a TLRMS. Due to its simple design and ease of use, the standard PID controller is widely employed; nonetheless, it frequently faces difficulties in complicated and unexpected contexts [32].

Proportional (P), integral (I), and derivative (D) control actions are combined to operate traditional PID controllers. While the proportional component (P) can raise overshoot but also helps to reduce steady-state errors, the derivative component (D) is in charge of lowering overshoot and speeding up settling time. While the integral component (I) decreases rising time and fixes steady-state faults, it also has the potential to cause overshoot and settling time to increase. PID controllers are widely used in industrial settings, however they can have trouble adjusting to dynamic or nonlinear systems. FONPID controllers have been offered as a solution to this problem enhancing the robustness and adaptiveness. FONPID controllers offer a type of adaptive control by dynamically adjusting the integral time and gains in response to control mistakes. The FONPID controller may adjust the gains for the proportional and integral components in real time, providing a more adaptable response to the nonlinear behaviour of the system, by employing nonlinear hyperbolic functions. Fractional-order controllers provide higher levels of precision in systems with more degrees of freedom, such as the three-link manipulator system, by introducing fractional-order operators for differentiation and integration. This method has been successfully used in control systems, providing more accurate and flexible control. The FO operators for D and I control actions are generated using the Oustaloup approximation method [33], guaranteeing precise and seamless control responses. To attain the best control performance, the approximation's parameters – such as the higher frequency ω_h and lower frequency ω_l – are are carefully chosen.

More sophisticated control techniques are made possible by these FO elements, as shown by the differential formulation of the FONPID (Fig. 2) [29, 34-38]. The purpose of this work is to demonstrate the benefits of FONPID controllers over conventional PID and NPID controllers, especially in the dynamic and complicated settings found in robotic manipulator systems.

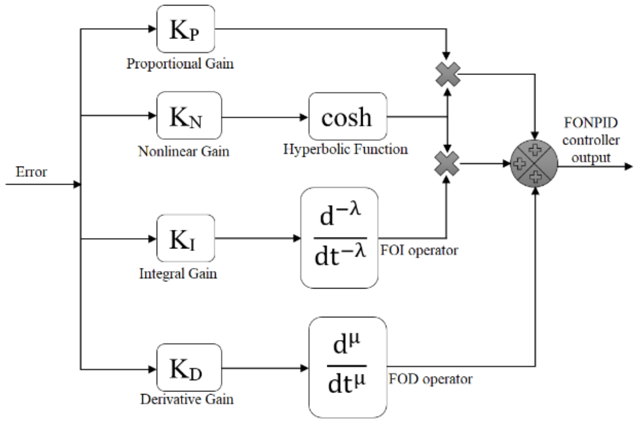

Fig. 2. FONPID control structure

$$u_{FONPID}(t) = K_Pe(t)f(e) + K_I\frac{d^{-\lambda}}{dt^{-\lambda}}f(e)e(t)dt + K_D\frac{d^{\mu}}{dt^{\mu}}e(t) \quad (20)$$

$$f(e) = \cosh(K_Ne) \quad (21)$$

or

$$f(e) = \frac{\exp(K_Ne) + \exp(-K_Ne)}{2} \quad (22)$$

where

$$e = \begin{cases} e\,;\ |e| \le e_{max} \\ e_{max} \times \mathrm{sgn}(e)\,;\ |e| > e_{max} \end{cases} \quad (23)$$

K_N, e_{max} are assumed as positive constant values. The lower limit of $f(e)$ is considered to be 1 for $e = 0$ [32-34].

To attain optimal control performance, a FONPID controller must be implemented, which requires the adjustment of five essential gains. Together with nonlinear gains, these gains also contain the proportional, integral, derivative, fractional-order integral, and fractional-order derivative operators. The goal of adjusting these gains is to make sure the controller maintains accuracy and robustness while reacting to system dynamics in an efficient manner. The CSA is used to achieve this tweaking. Cuckoo-inspired nesting behaviour (CSA) is an optimisation technique that draws inspiration from nature and is well-known for its ability to solve intricate optimisation problems. The algorithm minimises an objective function in an attempt to determine the best set of gains for the FONPID controller. The weighted sum of the Integrals of Square Error (ISE) and Integrals of Absolute Change in Controller Output (IACCO) define this objective function. When combined, these measures show the controller's accuracy as well as how smoothly its control actions flow. The CSA algorithm is applied to maximise the benefits of the FONPID controller by utilising the J_{min} function. The process is illustrated in Eqn. (24) and further explained in Fig. 3.

$$J_{min} = w_1 \times ISE + w_2 \times IACCO \tag{24}$$

Here, *ISE* is increased by w_1 and *IACCO* is increased by w_2. The values of w_1 and w_2 are 0.999 and 0.001, respectively [31].

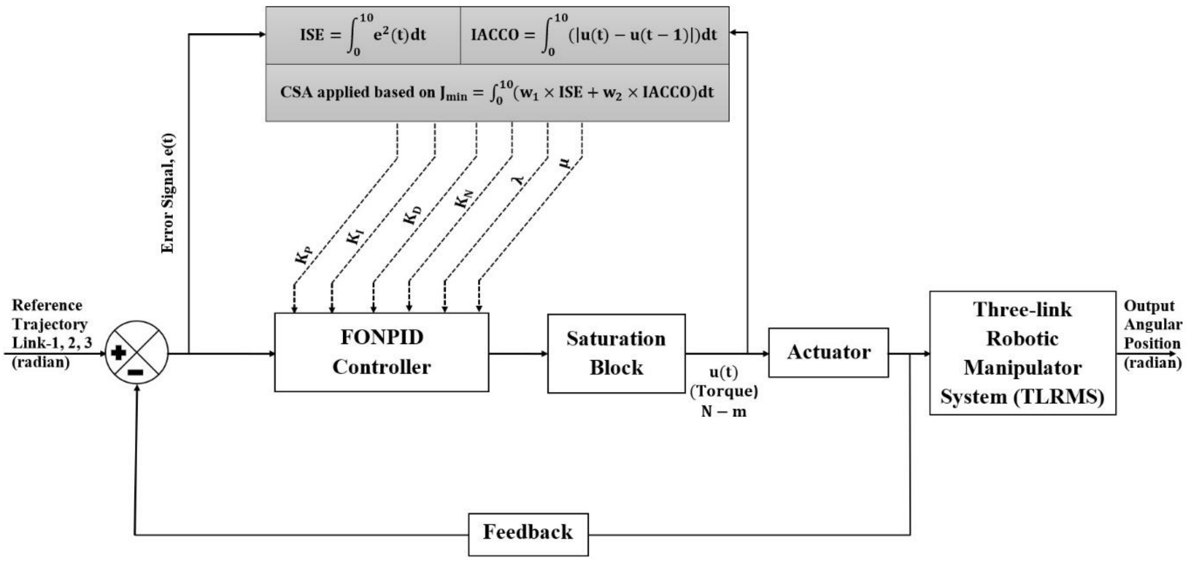

Fig. 3. Closed loop control configuration of CSA-tuned FONPID controller incorporated into TLRMS

With this method, the controller is guaranteed to be customised to the unique features and requirements of the TLRMS. A balance between minimal inaccuracy, respon-siveness, and stability can be achieved through the tuning process. Utilising the CSA, one can adjust the gains of a FONPID controller by concentrating on the fractional-order parameters λ and μ as well as K_P (proportional gain), K_I (integral gain), K_D (derivative gain), and K_N (nonlinear gain). The main elements of CSA for adjusting FONPID controller gains are summed up in the following steps, which also balance exploration and exploitation to identify the optimal course of action and providing good optimization as compared to other algorithms such as genetic algorithm (GA) and particle swarm optimization algorithm (PSO). According to preliminary research, CSA fared better at minimising the objective function and avoiding local optima than GA and PSO. CSA was the best option for this investigation because GA and PSO, despite their effectiveness, had slower convergence and more sensitivity to local optima in complex areas.

Step 1: Initialization

Several "nests" are generated, each of which represents a collection of gains for the FONPID controller. Random initial solutions are generated within the stated lower and upper bounds of the gains.

Step 2: Come up with novel solutions

Step sizes are obtained from a Levy distribution, and CSA uses Levy flights to generate new solutions. The bounds impose constraints on these new solutions.

Step 3: Assess and choose the finest

An objective function, usually based on the ISE or the IACCO, is used to evaluate new solutions. A new solution takes the place of the old one if it is more fit. The best-performing solution is updated in the bestnest.

Step 4: Discovery and randomization

The number of nests that are replaced with new ones is determined by a discovery rate (p_a), which adds diversity to the search process to prevent premature convergence.

Step 5: Termination and convergence

When a convergence criterion – such as obtaining minimum fitness or maximum iteration count – is satisfied, CSA continues to repeat. The FONPID controller is then equipped with the optimal gains.

An extra degree of precision and flexibility is offered by the FONPID controller's incorporation of FO operators. The controller's behaviour can be fine-tuned with the help of these operators, improving its ability to represent the dynamics of intricate systems. The system performs betterand is more resilient as a result, exhibiting improved adaptation to changing circumstances and a decreased chance of instability. All things considered, utilising CSA to fine-tune the FONPID controller and adding fractional-order operators results in a more reliable and effective control scheme for the TLRMS. By enhancing trajectory tracking, lowering steady-state error, and producing smoother control actions, this method can eventually result in a robotic system that is more dependable.

4 Simulation results and comparative performance analysis

MATLAB/SIMULINK was used for all simulations and comparison analyses. The machine has an Intel CoreTM i5 CPU running at 2.7 GHz, 8 GB of RAM, and a 32-bit operating system. The ordinary differential equation (ODE) was solved using the fourth-order Runge-Kutta method in the simulations, which employed a sampling rate of one millisecond. The continuous performance gains attained through optimisation throughout the study show how reliable the FONPID controller is. A minimum objective function criterion, J_{min}, was used to assess the performance of the FONPID, FOPID, and conventional PID controllers. All the controllers are optimized under the identical conditions. The findings are listed in Tab. 2. Figure 4 displays the relevant J_{min} curve for each type of controller. Table 3 lists the gain values for each controller. The FONPID controller beat the FOPID and PID controllers in terms of control precision and trajectory tracking, as seen in Tab. 2, where it obtained the lowest J_{min} value. The corre-sponding bar chart is represented in Figs. 5, 6 and 7 for ISE, IACCO and J_{min} values respectively.

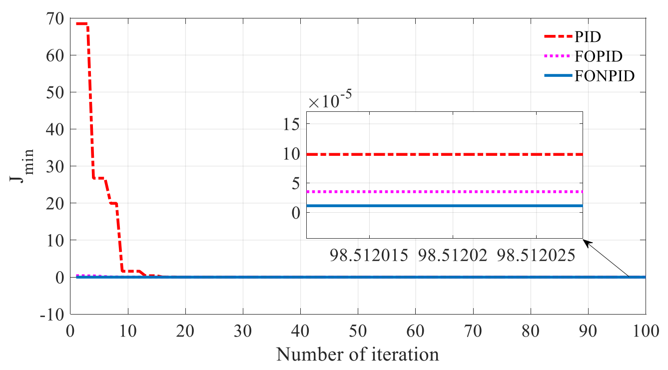

Fig. 4. $J_{\min}$ vs Number of iterations for FONPID, FOPID, PID controllers

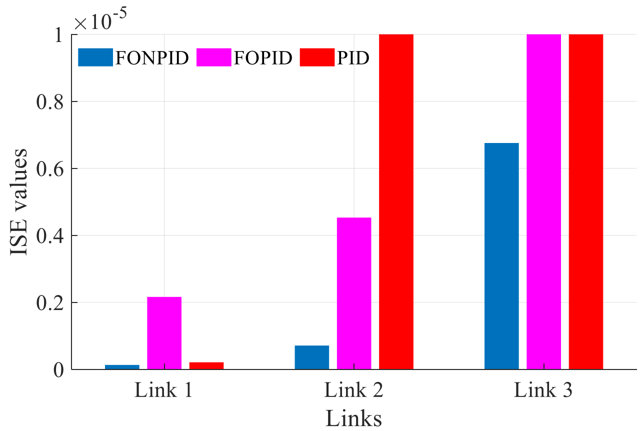

Fig. 5. ISE values of FONPID, FOPID, PID controllers

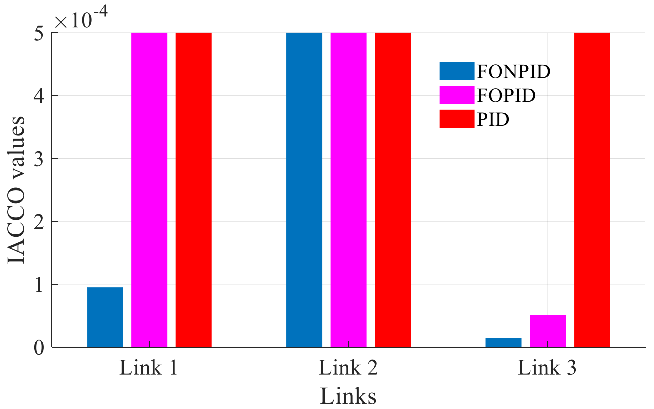

Fig. 6. IACCO values of FONPID, FOPID, PID controllers

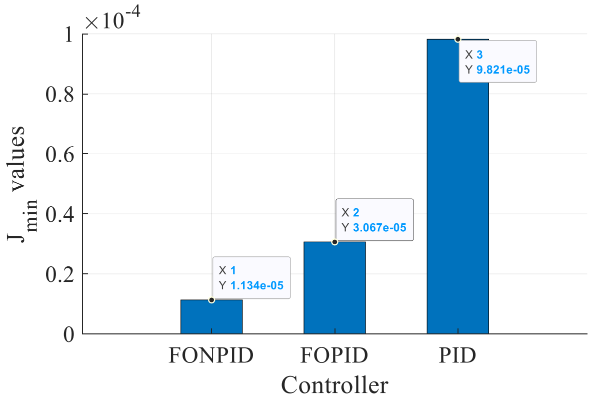

Fig. 7. J_{min} values for FONPID, FOPID, PID controllers

Table 2. $J_{\min}$ values along with ISE and IACCO metrics for FONPID, FOPID, PID controllers

Controller	ISE values			IACCO values			$J_{\min}$
	L1	L2	L3	L1	L2	L3	
FONPID	1.246×10^{-7}	7.025×10^{-7}	6.749×10^{-6}	9.45×10^{-5}	0.001773	1.426×10^{-5}	1.1338×10^{-5}
FOPID	2.155×10^{-6}	4.522×10^{-6}	1.234×10^{-5}	0.01	0.001759	5.019×10^{-5}	3.0666×10^{-5}
PID	2.042×10^{-7}	6.036×10^{-5}	0.00508	0.01	0.0009846	0.01	9.8208×10^{-5}

Table 3. Gain values for FONPID, FOPID, PID controllers

Controller		Gain values					
		K_P	K_N	K_I	K_D	λ	μ
FONPID	L1	100	500	90.9208	–93.0618	0.9	0.1283
	L2	4.6302	1	98.7440	20.7217	0.7782	0.1822
	L3	97.4802	441.6217	–16.4636	10.1036	0.1251	0.100
FOPID	L1	–92.3467	--	95.4384	86.9761	0.8997	0.2753
	L2	–100	--	35.6189	96.9612	0.8686	0.1141
	L3	–19.2866	--	46.8068	89.3663	0.8431	0.5803
PID	L1	19.7259	--	203.5010	2.9672	--	--
	L2	24.3084	--	162.2512	9.3600	--	--
	L3	35.5187	--	66.9255	120.4801	--	--

Figure 8, which shows the FONPID controller's trajectory tracking ability in the absence of disturbances and overall control results, also reflects this increased performance. For all links, the torque limit was set to [–10, 10] Nm in order to preserve control within these limitations. Figure 9 displays the error curve across the various controllers, showing that the FONPID controller achieved lower error than the other controllers. The controller output for each of the three links is shown in Fig. 10, further demonstrating the FONPID controller's improved performance. Because of its fractional-order operators and adaptive control capabi-lities, the research indisputably demonstrates that the FONPID controller is a better option for a three-link manipulator system. It provides more precise and reliable control, making it a great choice for complex manipulator applications. The results show that the FONPID controller is better suited to govern the dynamics of complex systems because it provides more stability, accuracy, and robustness.

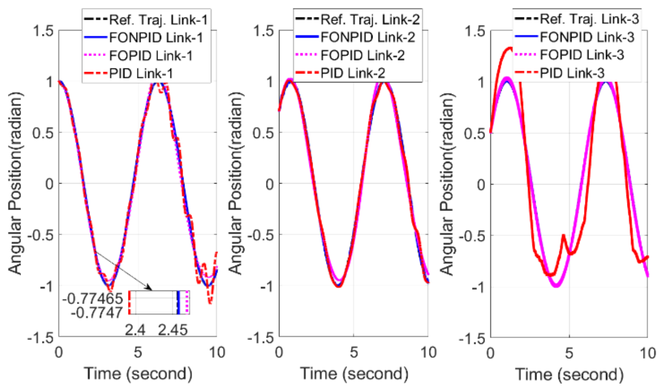

Fig. 8. Reference tracking curves of Link1, Link2, and Link3 for FONPID, FOPID, PID controllers

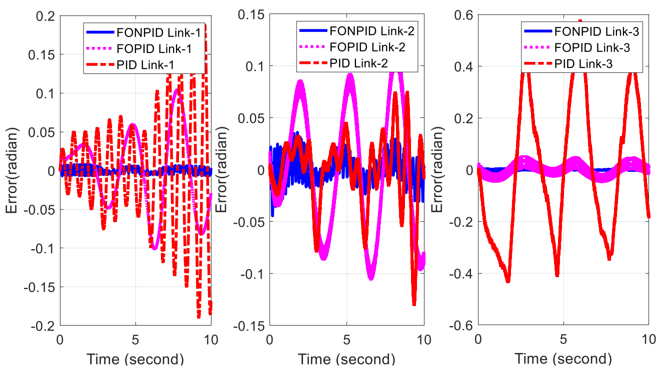

Fig. 9. Error signal for trajectory tracking analysis of Link1, Link2, and Link3 for FONPID, FOPID, PID controllers

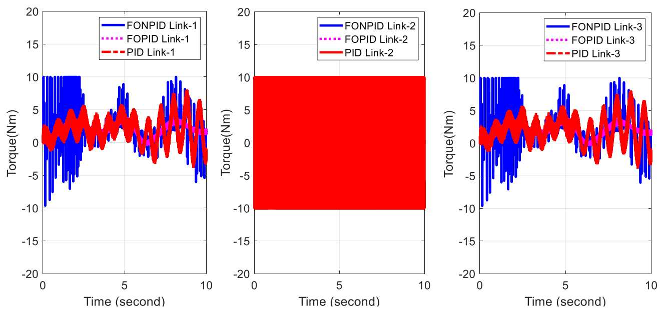

Fig. 10. Controller output curve for reference tracking of Link1, Link2, and Link3 for FONPID, FOPID, PID controllers

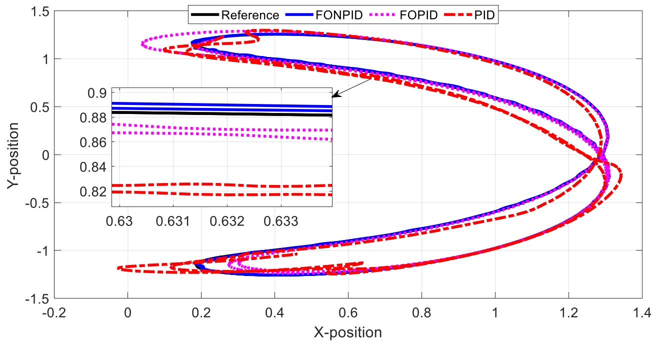

Fig. 11. X-Y curve for reference tracking study at system's input

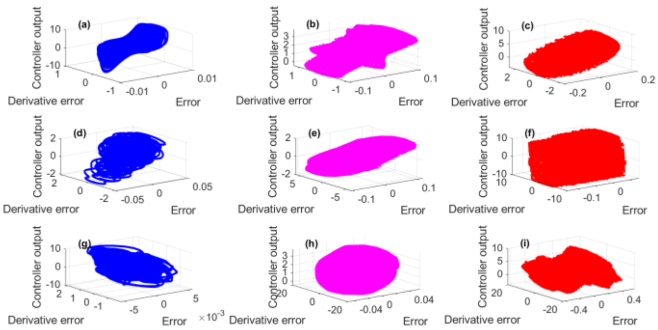

Fig. 12. Error, differential error and controller output (3D) curves of Link1, Link2, and Link3 for FONPID, NPID, PID controllers

As a result of its optimised gains driven by the J_{min} objective function criteria, the FONPID controller beats both the normal PID and FOPID controllers, according to the simulation findings and comparison analysis. The TLRMS's reference-tracking capability is greatly enhanced by the FONPID control action, guaranteeing precise tracking and efficient control. Throughout the simulations, which were carried out using the predetermined software configuration, the study carefully evaluated the planned trajectories and torque constraints. Achieving smooth trajectory tracking while reducing the influence of any outside disturbances was a primary goal. The X-Y curve for the reference-tracking investigation is shown in Fig. 11, which demonstrates the manipulator's ability to travel along the intended path.

Furthermore, Fig. 12 compares the trajectory tracking performance of FONPID, FOPID, and PID controllers using 3D response curves that display the error, differential error, and the controller output performance for Links 1, 2, and 3. The improved performance of the FONPID controller is demonstrated clearly by these visualisations. Based on simulation results, trajectory tracking is significantly improved by the FONPID controller. In terms of the J_{min} metric, it specifically obtained estimated performance increases of 63.03% and 88.45% in comparison to the FOPID and PID controllers, respectively. This significant improvement in performance highlights how well the FONPID controller works to provide accurate and consistent control in TLRMS.

5 Conclusion and future aspects

One of the biggest challenges for researchers is to control and regulate nonlinear systems with multi-input multi-output (MIMO) features, like three-link robotic manipulator systems (TLRMS). In this research, a fractional-order (FO) nonlinear PID (FONPID) controller is used to propose a robust and adaptive control technique for a TLRMS. The study compared the FOPID along with PID controllers to assess the efficacy of the FONPID controller in terms of reference tracking, and proper control behaviour of TLRMS. The trajectory tracking analysis's findings showed that the FONPID controller performed noticeably better than the FOPID and PID controllers. The FONPID controller demonstrated its superior control capabilities by attaining reductions in the objective function (J_{min}) of 63.03% and 88.45%, respectively, indicating considerable improvements. Based on this detailed analysis, it can be concluded that the FONPID controller is a very good way to control complicated MIMO systems, such as the three-link robotic manipulator. By illustrating the FONPID controller's apacity to manage the complexity of linked, nonlinear multi-input multi-output systems, the study advances the subject of control theory.

Subsequent investigations may concentrate on implementing the FONPID controller in increasingly intricate manipulator systems and evaluating its efficacy in practical situations. Given this controller's performance in the current investigation, there is a good chance that it will find wider use in robotics and control systems.

References

[1] J. J. Craig, *Introduction to robotics*. Pearson Educacion, 2006.

[2] S. S. Ge, “Advanced control techniques of robotic manipulators,” in *Proceedings of the 1998 American Control Conference. ACC (IEEE Cat. No.98CH36207)*, 1998, vol. 4, pp. 2185–2199 vol.4, doi: 10.1109/ACC.1998.703015.

[3] J. Wang and A. Chortos, “Control Strategies for Soft Robot Systems,” *Adv. Intell. Syst.*, vol. 4, no. 5, p. 2100165, May 2022, doi: https://doi.org/10.1002/aisy.202100165.

[4] I. B. Khallouf and D. S. Naidu, “Advanced Control Strategies for the Robotic Hand,” in *2018 IEEE 14th International Conference on Control and Automation (ICCA)*, 2018, pp. 698–703, doi: 10.1109/ICCA.2018.8444269.

[5] K. Bingi, B. Rajanarayan Prusty, and A. Pal Singh, “A Review on Fractional-Order Modelling and Control of Robotic Manipulators,” *Fractal and Fractional*, vol. 7, no. 1. 2023, doi: 10.3390/fractalfract7010077.

[6] A. Dzedzickis, J. Subačiūtė-Žemaitienė, E. Šutinys, U. Samukaitė-Bubnienė, and V. Bučinskas, “Advanced Applications of Industrial Robotics: New Trends and Possibilities,” *Applied Sciences*, vol. 12, no. 1. 2022, doi: 10.3390/app12010135.

[7] S. B. Niku, *Introduction to robotics: analysis, control, applications*. John Wiley & Sons, 2020.

[8] Y. Liu and P. Ben-Tzvi, “Design, Analysis, and Optimization of a New Two-DOF Articulated Multi-Link Robotic Tail.” Aug. 18, 2019, doi: 10.1115/DETC2019-97537.

[9] R. P. Borase, D. K. Maghade, S. Y. Sondkar, and S. N. Pawar, “A review of PID control, tuning methods and applications,” *Int. J. Dyn. Control*, vol. 9, no. 2, pp. 818–827, 2021, doi: 10.1007/s40435-020-00665-4.

[10] H. Seraji, “A new class of nonlinear PID controllers with robotic applications,” *J. Robot. Syst.*, vol. 15, no. 3, pp. 161–181, Mar. 1998, doi: https://doi.org/10.1002/(SICI)1097-4563(199803)15:3<161::AID-ROB4>3.0.CO;2-O.

[11] W. Yu, X. Li, and R. Carmona, “A novel PID tuning method for robot control,” *Ind. Robot An Int. J.*, vol. 40, no. 6, pp. 574–582, Jan. 2013, doi: 10.1108/IR-09-2012-406.

[12] J. G. Batista *et al.*, “Performance Comparison Between the PID and LQR Controllers Applied to a Robotic Manipulator Joint,” in *IECON 2019 - 45th Annual Conference of the IEEE Industrial Electronics Society*, 2019, vol. 1, pp. 479–484, doi: 10.1109/IECON.2019.8927059.

[13] A. J. Moshayedi, A. Roy, and A. Kolahdooz, “PID Tuning Method on AGV (automated guided vehicle) Industrial Robot,” *Journal of Simulation and Analysis of Novel Technologies in Mechanical Engineering*, vol. 4, no. 1. School of Information Engineering, Jiangxi University of Science and Technology,No 86, Hongqi Ave, Ganzhou, Jiangxi,341000, China, pp. 53–66, 1398, [Online]. Available: http://sanad.iau.ir/fa/Article/1091957.

[14] R. Benotsmane and G. Kovács, “Optimization of Energy Consumption of Industrial Robots Using Classical PID and MPC Controllers,” *Energies*, vol. 16, no. 8. 2023, doi: 10.3390/en16083499.

[15] J. Kumar, V. Kumar, and K. P. S. Rana, “Study of optimization methods for tunning SOFC gains for manipulator control,” in *2015 Annual IEEE India Conference (INDICON)*, 2015, pp. 1–6, doi: 10.1109/INDICON.2015.7443832.

[16] R. Sharma, P. Gaur, and A. P. Mittal, “Performance evaluation of cuckoo search algorithm based FOPID controllers applied to a robotic manipulator with actuator,” in *2015 International Conference on Advances in Computer Engineering and Applications*, 2015, pp. 356–363, doi: 10.1109/ICACEA.2015.7164730.

[17] R. Sharma, P. Gaur, and A. P. Mittal, “Performance analysis of two-degree of freedom fractional order PID controllers for robotic manipulator with payload,” *ISA Trans.*, vol. 58, pp. 279–291, 2015, doi: https://doi.org/10.1016/j.isatra.2015.03.013.

[18] L. Zhang, L. Liu, and S. Zhang, “Design, Implementation, and Validation of Robust Fractional-Order PD Controller for Wheeled Mobile Robot Trajectory Tracking,” *Complexity*, vol. 2020, p. 9523549, 2020, doi: 10.1155/2020/9523549.

[19] G. Singh and V. K. Banga, “Kinematics and trajectory planning analysis based on hybrid optimization algorithms for an industrial robotic manipulators,” *Soft Comput.*, vol. 26, no. 21, pp. 11339–11372, 2022, doi: 10.1007/s00500-022-07423-y.

[20] K. Patel, V. Kalaichelvi, R. Karthikeyan, and S. Bhattathiri, “Modelling, Simulation and Control of Incremental Sheet Metal Forming Process using CNC Machine Tool,” *Procedia Manuf.*, vol. 26, pp. 95–106, 2018, doi: https://doi.org/10.1016/j.promfg.2018.07.012.

[21] R. Sharma, K. P. S. Rana, and V. Kumar, “Performance analysis of fractional order fuzzy PID controllers applied to a robotic manipulator,” *Expert Syst. Appl.*, vol. 41, no. 9, pp. 4274–4289, 2014, doi: 10.1016/j.eswa.2013.12.030.

[22] Sweta, J. Kumar, and V. K. Deolia, “Investigation of Fractional-Order Nonlinear PID Controller for Three-link Robotic Manipulator System,” in *2023 14th International Conference on Computing Communication and Networking Technologies (ICCCNT)*, 2023, pp. 1–7, doi: 10.1109/ICCCNT56998.2023.10307476.

[23] V. Mohan, H. Chhabra, A. Rani, and V. Singh, “Robust self-tuning fractional order PID controller dedicated to non-linear dynamic system,” *J. Intell. Fuzzy Syst.*, vol. 34, pp. 1467–1478, 2018, doi: 10.3233/JIFS-169442.

[24] A. Kumar, P. J. Gaidhane, and V. Kumar, “A nonlinear fractional order PID controller applied to redundant robot manipulator,” in *2017 6th International Conference on Computer Applications In Electrical Engineering-Recent Advances (CERA)*, 2017, pp. 527–532, doi: 10.1109/CERA.2017.8343385.

[25] D. Gupta, V. Goyal, and J. Kumar, “Comparative performance analysis of fractional-order nonlinear PID controller for complex surge tank system: tuning through machine learning control approach,” *Multimed. Tools Appl.*, 2024, doi: 10.1007/s11042-024-18427-1.

[26] P. Tripathi, J. Kumar, and V. K. Deolia, “Trajectory Tracking Analysis of Fractional-Order Nonlinear PID Controller for Single Link Robotic Manipulator System BT - Proceedings of Fourth International Conference on Computer and Communication Technologies,” 2023, pp. 443–452.

[27] J. Kumar, V. Goyal, and D. Gupta, “Reliable Incorporation of Robust Fractional-Order Nonlinear PID Controller into Integrated Power System Using Gray Wolf Optimization Method BT - Advances in Data and Information Sciences,” 2023, pp. 333–343.

[28] J. Kumar, V. Kumar, and K. P. S. Rana, “A fractional order fuzzy PD+I controller for three-link electrically driven rigid robotic manipulator system,” *J. Intell. Fuzzy Syst.*, vol. 35, pp. 5287–5299, 2018, doi: 10.3233/JIFS-169812.

[29] T. Kathuria, A. Gupta, J. Kumar, V. Kumar, and K. P. S. Rana, “Study of optimization methods for tuning of PID gains for three link manipulator,” *2017 7th Int. Conf. Cloud Comput. Data Sci. Eng. - Conflu.*, 2017.

[30] J. Kumar, D. Gupta, and V. Goyal, “Nonlinear PID Controller for Three-Link Robotic Manipulator System: A Comprehensive Approach BT - Proceedings of International Conference on Communication and Artificial Intelligence,” 2022, pp. 137–152.

[31] J. Kumar, V. Kumar, and K. P. S. Rana, “Fractional-order self-tuned fuzzy PID controller for three-link robotic manipulator system,” *Neural Comput. Appl.*, vol. 32, no. 11, pp. 7235–7257, 2020, doi: 10.1007/s00521-019-04215-8.

[32] A. Agrawal, V. Goyal, and P. Mishra, “Adaptive control of a nonlinear surge tank-level system using neural network-based PID controller,” *Adv. Intell. Syst. Comput.*, vol. 698, pp. 491–500, 2019, doi: 10.1007/978-981-13-1819-1_46.

[33] A. Agrawal, “Analysis of Efficiency of Fractional Order Technique in a Controller for a Complex Nonlinear Control Process BT - Proceedings of International Conference on Big Data, Machine Learning and their Applications,” 2021, pp. 1–11.

[34] V. Goyal, P. Mishra, and V. Kumar, “A Robust Fractional Order Parallel Control Structure for Flow Control using a Pneumatic Control Valve with Nonlinear and Uncertain Dynamics,” *Arab. J. Sci. Eng.*, 2018, doi: 10.1007/s13369-018-3328-6.

Received 14 May 2024